Pegylated Phosphotidylethanolamine Inhibiting P-Glycoprotein Expression and Enhancing Retention of Doxorubicin in MCF7/ADR Cells

JING WANG,[1] HUI QU,[1] LINGTAO JIN,[1] WENFENG ZENG,[1] LEI QIN,[1] FAYUN ZHANG,[1] XIULI WEI,[1] WANLIANG LU,[2] CHUNLING ZHANG,[1] WEI LIANG[1]

[1]Protein and Peptide Pharmaceutical Laboratory, National Laboratory of Biomacromolecules, Institute of Biophysics, Chinese Academy of Sciences, Beijing 100101, China

[2]School of Pharmaceutical Sciences, Peking University, Beijing, 100083, China

Received 24 September 2010; revised 16 November 2010; accepted 20 November 2010

Published online 18 January 2011 in Wiley Online Library (wileyonlinelibrary.com). DOI 10.1002/jps.22461

ABSTRACT: The failure of the clinical treatment of cancer patients is often attributed to drug resistance of the tumor to chemotherapeutic agents. P-glycoprotein (P-gp) contributes to drug resistance via adenosine 5′-triphosphate (ATP)-dependent drug efflux pumps and is widely expressed in many human cancers. Up to date, a few of nanomaterials have shown the effects on P-gp function by different ways. To study the mechanism of the increased cytotoxicity of doxorubicin (DOX) by pegylated phosphotidylethanolamine (PEG-PE) in drug-resistant cancer cells, a series of *in vitro* cell assays were performed, including identification of P-gp function, quantitative studies on uptake and efflux of DOX, inhibitory effects of blank PEG-PE micelles on mRNA and protein levels of P-gp, and intracellular ATP content alteration. Finally, combining MDR-1 RNA interference (siRNA) with DOX encapsulated in PEG-PE micelles (M-DOX) to improve cytotoxicity of DOX was also studied. M-DOX showed fivefold lower the concentration that caused 50% killing tumor cellthan that of free DOX in the P-gp-overexpressing MCF-7 breast cancer (MCF-7/ADR) cells. M-DOX enhanced the cellular uptake and retention of DOX in MCF-7/ADR cells. PEG-PE block molecules can inhibit P-gp expression through downregulating *MDR-1* gene. Cytotoxicity of M-DOX was further improved by knocking down the *MDR-1* gene using siRNA in the multidrug-resistant cells. We conclude that the increased cytotoxicity of DOX encapsulated in PEG-PE micelle is due to the reduced P-gp expression by PEG-PE block molecules, and accordingly enhancing the cellular accumulation of DOX. To overcome drug resistance of tumor cells, the combination of nanotechnology and biotechnology could be an effective strategy such as PEG-PE formed micelles and siRNA. © 2011 Wiley-Liss, Inc. and the American Pharmacists Association J Pharm Sci 100:2267–2277, 2011

Keywords: P-glycoprotein; PEG-PE; Polymeric drug carrier; Micelle; multidrug resistance; MDR-1 siRNA; doxorubicin; Cancer chemotherapy.

INTRODUCTION

The failure of the clinical treatment of cancer patients is often attributed to drug resistance of the tumor to chemotherapeutic agents.[1] Multidrug resistance (MDR) has become a severe barrier for chemotherapy to exert an antineoplastic effect in most common malignancies. Among various mechanisms of MDR, the reduced accumulation of antitumor drug is most commonly seen.[2] P-glycoprotein (P-gp), together with MDR-associated proteins (MRP1 and MRP2), the breast cancer resistance protein (BCRP), and so

Abbreviations used: PEG-PE, pegylated phosphotidylethanolamine; DOX, doxorubicin; P-gp, P-glycoprotein; M-DOX, doxorubicin encapsulated in PEG-PE micelles; F-DOX, free doxorubicin; siRNA, RNA interference; MCF-7/ADR, P-gp-overexpressing MCF-7 breast cancer; RT-PCR, reverse transcriptase-polymerase chain reaction.

Correspondence to: Wei Liang (Telephone: +86-10-648-898-61; Fax: +86-10-648-675-66; E-mail: weixx@sun5.ibp.ac.cn); Chunling Zhang (Telephone: 86-10-648-453-88; Fax: 86-10-648-453-88; E-mail: zhangcl@moon.ibp.ac.cn)

Jing Wang and Hui Qu contributed equally to this work.

Journal of Pharmaceutical Sciences, Vol. 100, 2267–2277 (2011)

on, contributes to drug resistance via adenosine 5′-triphosphate (ATP)-dependent drug efflux pumps and is widely expressed in many human cancers, including cancers of the gastrointestinal tract, cancers of the hematopoietic system, cancers of the genitourinary system, and childhood cancers.[3,4]

As the most common membrane drug efflux transporter, P-gp significantly reduces intracellular levels of various structurally differed compounds, including doxorubicin (DOX), a broad-spectrum cytotoxic anticancer drug commonly included in the regimens of breast cancer treatment. Clinical data show that this transporter has been detected in 63% of patients with untreated breast cancer.[5] An increase in P-gp expression in breast cancer after chemotherapy has also been correlated with lower clinical response rates.[6,7] These observations indicate that the activity of P-gp efflux pump seems to be one of the most influential factors in resistant breast cancer treatment.

In the past years, nano-sized formulation strategies, such as folate-targeted liposomes,[8,9] pH-sensitive micelles,[10,11] and solid lipid nanoparticles, have been developed to potentially address P-gp-mediated drug resistance.[12–16] These delivery systems have been shown to decrease the resistance of P-gp-expressing cells *in vitro*, which is due to increased cellular accumulation of the drug. However, intracellular drug was still pumped by P-gp efflux because these formulations did not affect P-gp function. Up to date, a few of nanomaterials have shown the effects on P-gp function by different ways. Polyethyleneglycol-660 hydroxystearate inhibited P-gp-related drug transport.[17,18] Fatty acid–PEG diesters interfered with P-gp substrate binding.[19,20] Pluronic micelles composed of poly(oxyethylene)–poly(oxypropylene) and Brij 78 (polyoxyethylene 20-stearylether)-based nanoparticals have been used to selectively inhibit the P-gp function by ATP depletion.[21,22] Proposed mechanisms for some conjugates, such as N-(2-hydroxypropyl) methacrylamide, have included internalization by endocytosis and partial inhibition of *P-gp* gene expression.[23]

Here, we described a new strategy to overcome MDR by DOX loaded into pegylated phosphotidylethanolamine (PEG-PE) micelles (M-DOX) that showed higher cytotoxicity than free DOX (F-DOX), without any chemical ligand decoration, and had an ability to partially reverse DOX resistance in MCF-7/ADR cells. As it was shown in our previous study,[24] this micelle delivery system effectively enhanced *in vitro* and *in vivo* antitumor efficacy of DOX in nonresistant lung cancer. The evaluation of M-DOX performance in resistant breast cancer cells and exploration of related mechanism will help us better understand the micelle intracellular activity and provide useful reference for further design of nano-sized drug delivery system in resistant cancer treatment.

EXPERIMENTAL

Materials

PEG2000-DSPE was purchased from Avanti Polar Lipids (Alabaster, Alabama); DOX was kindly provided by HaiZheng Corp. (Taizhou, China); triethylamine, chloroform, rhodamine123, and verapamil were purchased from Sigma–Aldrich (St. Louis, Missouri); and methanol was purchased from Merck (Darmstadt, Germany).

Cell Culture

Sensitive human breast cancer cell line (MCF-7) and multidrug-resistant cell line (MCF-7/ADR) were granted by Academy of Military Medical Sciences. Cells were grown in Dulbecco's modified Eagle's medium (DMEM) (Gibco, New York) supplemented with 10% fetal bovine serum (PAA, Pasching, Austria), 100 units/mL penicillin, and 100 units/mL streptomycin.

Reverse Transcriptase-Polymerase Chain Reaction

To compare the mRNA expression of the multidrug-resistant genes in different types of cancer cells, total RNAs were isolated from MCF-7 and MCF-7/ADR cells using TRIzol (Invitrogen, California). To address the effect of blank PEG-PE micelles on the mRNA expression of the multidrug-resistant genes, RNAs were also isolated from MCF-7/ADR cells treated with blank micelles 6.8 or 34 μM, respectively. The mRNAs were reversely transcribed to complementary DNAs by M-MLV reverse transcriptase (RT) (Invitrogen). All the primers were purchased from Invitrogen. Primers for human MDR1: 5′-AAAGCTGTC AAGGAAGCCAA-3′ and 5′-TGACTCC ATCATCGAAACCA-3′, MRP1: 5′-ATGTCACGTGG AATACCAGC-3′ and 5′-GAAGACTGAACTCCCTT CCT-3′, MRP2: 5′-ACAGAGGCTGGTGGCAACC-3′ and 5′-ACCATTACCTTGTCACTGTCCATGA-3′, and BCRP: 5′-TGGCTGTCATGGCTTCAGTA-3′ and 5′-GCCACGTGATTCTTCCACAA-3′ were used. The primers for β-actin were sense primer 5′-CATGTACGTTGCTATCCAGGC-3′ and antisense primer 5′-CTCCTTAATGTCACGCACGAT-3′. After initial denaturation at 95°C for 5 min, polymerase chain reaction (PCR) was performed for 30 cycles (30 s at 94°C, 30 s at annealing temperature, and 40 s at 72°C) using Taq polymerase (TaKaRa, Dalian, China). Reaction products (20 μL per lane) were electrophoresed in 1% agarose, stained with ethidiumbromide and photographed.

Detection of P-gp Expression by Flow Cytometry

About 10^6 cells were trypsined, centrifuged, and resuspended in 100 μL staining buffer (DMEM added 2% fetal bovine serum and 0.1% NaN_3). Twenty microliters fluorescein isothiocyanate (FITC)-conjugated mouse antihuman monoclonal antibody (BD Biosciences) was added and incubated in the dark at 4°C for 30 min. Cells were centrifuged and washed once with phosphate-buffered saline (PBS), fluorescence intensity of FITC was analyzed by FACSCalibur with a 488-nm argon laser and 530-nm band pass filter.

Activities of P-gp

The activity of P-gp was determined by Rhodamine123 or DOX efflux assay. MCF-7/ADR cells were seeded in 12-well plates at a density of 10^5 per well and incubated with DMEM media containing 0.5 μM Rhodamine123 or 17 μM DOX in the presence of 20 μM verapamil for 1 h. Then, the cells were washed with PBS and further incubated with fresh DMEM media in the presence or absence of 20 μM verapamil for another 1 h. Finally, the cells were washed, trypsined, and harvested in ice-cold PBS and kept on ice until analysis. Intracellular fluorescence was detected in a Becton Dickinson FACSCalibur (San Jose, California) with a 488-nm argon laser. In each sample, at least 10^4 cells were counted. To quantify P-gp functional change, the ratio between the median fluorescence with and without P-gp inhibitor verapamil during the efflux period was calculated. The percentage of pumped drug is equal to one intracellular drug without verapamil/intracellular drug with verapamil.[25]

Cell Growth Inhibition Assay

Both MCF-7 and MCF-7/ADR cells were plated at a density of 5×10^3 cells per well in 100 μL DMEM medium in 96-well plates and grown for 24 h, respectively. Cells were exposed to a series of concentrations of F-DOX and M-DOX alone, F-DOX and M-DOX combined with 100 nM RNA interference (siRNA) MDR-1, or with verapamil for 48 h, and the viability of cells was measured using a methylthiazoletetrazolium (MTT) method. Briefly, 100 μL of MTT solution (0.5 mg/mL in PBS) was added to each well. The plates were incubated for 4 h at 37°C. After incubation, 100 μL of dimethyl sulfoxide (Sigma–Aldrich) was added to each well for 10 min at room temperature. Absorbance was measured at 570 nm using a plate reader (Thermo, Erlangen, Germany). The mean percentage of cell survival relative to that of untreated cells was estimated from data of three individual experiments. The concentration of DOX at which cell killing was 50% was calculated by curve fitting using SPSS software (version 12.0; SPSS Inc., Chicago, Illinois).

Quantification of DOX Internalization

The measurement of internalized DOX was performed as described previously.[24] Briefly, MCF-7/ADR cells were seeded in six-well plates at a concentration of 10^5 per well and incubated with M-DOX or F-DOX of a series of concentrations for desired time. Then, the cells were washed, trypsined, and collected in ice-cold PBS. The intracellular DOX was analyzed using a Becton Dickinson FACSCalibur cytometer, equipped with an argon laser (488 nm) and emission filter for 550 nm. Data collection involved 10,000 counts per sample. The data were analyzed using CELLQuest^{TM} software (BD Biosciences, Bedford, MA) and expressed as the geometric mean of the entire population. Cells incubated without DOX–polymer conjugates were used to account for the background fluorescence.

Cellular ATP Assay

MCF-7/ADR cells were seeded in 96-well plates at a density of 2000 per well and incubated with blank PEG-PE micelles (0 to 34 μM) at 37°C for 48 h. After treatment, the cells were washed with PBS, and intracellular ATP was determined using ATP assay kit (Promega, Beijing, China) based on luminescence assay and normalized by an MTT absorbance.

Protein Extraction and Quantification

Cells 10^6 were lysed in 200 μL RAPI lysis buffer containing proteinase inhibitor cocktails in a final concentration of 10 μg/mL and kept on ice for 30 min. Total cell lysate was centrifuged at 12,000 × g for 5 min, and the supernatant was collected as cellular total proteins. Protein content was determined by BCA protein assay kit (Shenergy Biocolor, Beijing, China) using bovine serum albumin as a standard.

Detection of P-gp Expression by Western Blotting

Expression of P-gp in MCF-7/ADR cells was verified by western blotting analysis. Proteins were separated by SDS–PAGE and transferred to 0.45 μm nitrocellulose membrane. Then, the proteins were blocked by incubation in Tris-buffered saline containing 0.1% Tween 20 and 5% skim milk for 1 h at room temperature in the shaker. Subsequently, the immunoblot analysis were performed with an anti-P-gp monoclonal antibody(Santa Cruz Biotechnology, Santa Cruz, California; dilution 1:500) or anti-β-actin monoclonal antibody (Santa Cruz Biotechnology; dilution 1:500) diluted in blocking buffer overnight at 4°C. After washing extensively, the blots were incubated with goat antimouse antibody conjugated to horseradish peroxidase (Santa Cruz Biotechnology; dilution 1:1000) for 1 h at room temperature in the shaker.

Bands were visualized by enhanced chemiluminescence using the ECL plus kit (Applygen, Beijing, China).

MDR-1 siRNA Transfection

P-glycoprotein silencing Si1 (21 nt) were synthesized targeting the human MDR-1 mRNA at the region 88–108 nt relative to the start codon (sense strand5′-GAAACCAACUGUCAGUGUA) by Invitrogen Company. A scrambled Si1–Si2 was synthesized as a negative control (sense strand 5′-GAUACGAAUUGACACCGUA). Cells (3×10^5/well) were grown in six-well plates to 30%–40% confluence and then be transfected by 100 nM siRNA with Lipofectamine2000 (Invitrogen, California) according to manufacturer guideline. After 5 h incubation in serum-free DMEM at 37°C, completed DMEM with 10% FBS were added. The cells were incubated with DMEM at 37°C for 48 or 72 h.

Statistical Analysis

Data and results are reported as means ± SD unless noted otherwise. The differences of the variables between groups were performed with the Student's *t*-test using SPSS 11.0 program. *P* values less than 0.05 were considered to be statistically significant.

RESULTS

Overexpression and High Activity of P-gp in MCF-7/ADR Cells

Tumor cells overexpressing multidrug export pumps, which are members of the family of ATP-binding cassette transport proteins, such as P-gp, MRP1, MRP2, and BCRP, may contribute to their resistance to chemotherapeutic agents.[26–28] Our results showed that mRNA expressions of *MRP-1*, *MRP-2*, and *BCRP* gene had the same level in both MCF-7 and MCF-7/ADR cells. However, *MDR-1* gene was expressed positively in MCF-7/ADR cells, whereas negatively in MCF-7 cells (Fig. 1a). *MDR-1* gene is translated to P-gp, which is responsible for pumping many small-molecule drugs and results in MDR. Thus, we measured the protein level of this gene using FITC-labeled antibody. Indeed, the level of P-gp in MCF-7/ADR cells was much higher than in MCF-7 cells (Fig. 1b).

To test P-gp activity, we measured the efflux of Rhodamine123 and F-DOX with or without verapamil, a well-known inhibitor of P-gp, blocks P-gp-modulated efflux of antitumor drugs in the cell.[29] Both Rhodamine123 and F-DOX are substrates of P-gp, the higher percentage of pumped drug indicates the higher P-gp activity. As shown in Figure 1c, in MCF-7 cells, the percentage of pumped Rhodamine123 and F-DOX was 24.8% and 8.1%, respectively, whereas in MCF-7/ADR cells, the percentage was up to 66.9% and 44.8%, respectively. These results indicate that P-gp has a high activity in MCF-7/ADR cells. Furthermore, we tested the cytotoxicity of F-DOX to these two cell lines by MTT, and calculated the concentration that caused 50% killing tumor cell (IC_{50}). The IC_{50} values were 2.7 ± 0.6 μM for MCF-7 cells and 72 ± 3.5 μM for MCF-7/ADR cells (Fig. 1d). These results indicate that overexpression and high activity of P-gp are contributed to drug resistance of MCF-7/ADR cells.

Enhancing Cytotoxicity of DOX-Encapsulated PEG-PE Micelles

To assess the effect of micellization on cytotoxic activity of DOX in MCF-7/ADR cells, we performed an MTT assay to determine the cellular viability after 2 h incubation with F-DOX or M-DOX followed by 72 h incubation in drug-free media (Fig. 2a). In the absence of verapamil, the IC_{50} value of F-DOX (72 ± 3.5 μM) was approximately fivefold higher than that of M-DOX (12.7 ± 1.2 μM). Compared with the absence of verapamil, the IC_{50} value of M-DOX was three times lower (4.2 ± 0.5 μM) and the IC_{50} value of F-DOX was five times lower (15.3 ± 1.0 μM) in the presence of verapamil (Fig. 2b). These results indicate that the encapsulation of DOX in PEG-PE micelles play an important role in the increasing DOX cytotoxicity. Moreover, verapamil has less effect on cytotoxicity of M-DOX, implying a change of P-gp function when the MCF-7/ADR cells exposed to M-DOX.

Rapid Internalization and Extending Cellular Retention of M-DOX

To compare the internalization dynamics of M-DOX with F-DOX, MCF-7/ADR cells were treated with 1.0 μM DOX for different times or with various concentrations of DOX for 1 h, and then the intracellular DOX was quantified by flow cytometry. In both time- and drug concentration-dependent conditions, M-DOX was internalized into cells more rapidly than F-DOX (Figs. 3a and 3b), indicating that micellization accelerated the cellular uptake of DOX.

Besides the rapid internalization, the enhanced retention of M-DOX in MCF-7/ADR cells was also observed. MCF-7/ADR cells were incubated with 3.4 μM DOX for 7 h, washed, and then incubated with DOX-free media for different hours with or without verapamil. As shown in Figures 4a and 4b, intracellular M-DOX was consistently higher than F-DOX. The enhanced cellular retention of M-DOX may be due to increasing internalization or decreasing efflux or both. To address this question, we compared the percentage of pumped DOX 10 h later (Fig. 4c). In the presence of verapamil, P-gp activity was inhibited, and there was no significant difference between F-DOX and M-DOX in the percentage of pumped DOX. However, in the absence of verapamil, the percentage of pumped

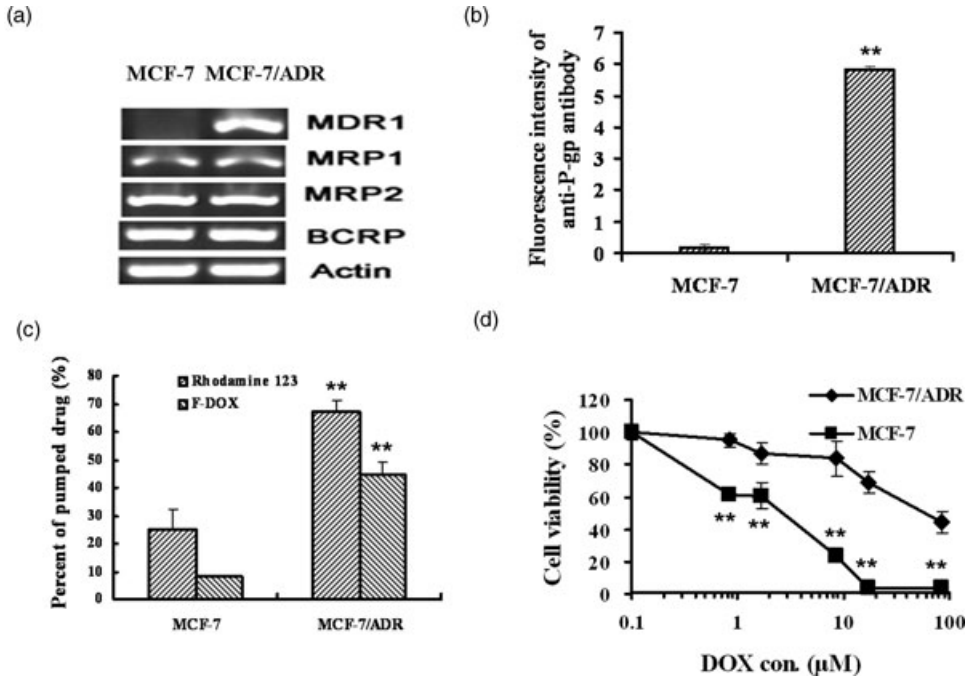

Figure 1. 1 Identification of P-gp activity. (a) Reverse-transcription PCR analysis of mRNA levels of MDR-1, MRP-1, MRP-2, BCRP in MCF-7 and MCF-7/ADR cells, β-actin used as a control. (b) P-gp expression detected by flow cytometry using FITC-conjugated anti-P-gp antibody in MCF-7/ADR and MCF-7 cells. Data represent mean ± SD ($n = 3$) for individual experiments. Columns, mean; Bars, SD. P-gp expression in MCF-7/ADR cells is higher than in MCF-7 cells ($^{**}P < 0.01$). (c) P-gp activity detected by flow cytometry in MCF-7 and MCF-7/ADR cells after 2 h treatment of Rhodamine123 (500 nM) and F-DOX (17 μM) in the presence of 20 μM verapamil for 1 h, washed and further incubated with drug-free media with or without 20 μM of verapamil for another 1 h. Data represent mean ± SD ($n = 3$) for individual experiments. Columns, mean; Bars, SD. P-gp activity in MCF-7/ADR cells is higher than in MCF-7 cells ($^{**}P < 0.01$). (d) Cytotoxic effects of F-DOX in MCF-7 cells and MCF-7/ADR cells measured by MTT. Cells were exposed to F-DOX ranging from 0 to 85 μM for 2 h and then incubated in drug-free media for 72 h. Data represent mean ± SD ($n = 3$) for individual experiments. MCF-7 cells are sensitive to F-DOX compared with MCF-7/ADR cells ($^{**}P < 0.01$).

M-DOX decreased by 10% as compare with F-DOX. This result indicates that P-gp activity in M-DOX-treated cells is reduced, and PEG-PE micelle alone may have an influence on the P-gp function.

Blank PEG-PE Micelles Inhibiting P-gp Activity in MCF-7/ADR Cells

P-glycoprotein activity was determined by the efflux of Rhodamine123 and F-DOX in MCF-7/ADR cells, and verapamil was used to inhibit the P-gp activity. As shown in Figure 5, approximately 67% of the intracellular Rhodamined123 was pumped out in the untreated cells. Both 6.8 and 34 μM of blank PEG-PE micelles reduced the percentage of pumped drug to 52% ($P < 0.05$) and 32% ($P < 0.01$), respectively. Efflux of F-DOX was also depressed by PEG-PE blank micelles in a concentration-dependent manner. Thirty-four micromolar of blank micelles resulted in a reduction of the percentage of pumped drug from 45% to 29% ($P < 0.05$). The decreased P-gp activity may result from the reduction of P-gp expression or the depletion of cellular ATP, thus resulting in an increase in the accumulation and the retention of M-DOX compared with F-DOX in MCF-7/ADR cells.

Effect of Blank PEG-PE Micelles on Intracellular ATP

P-glycoprotein is an ATP-dependent protein. Depleting cellular ATP would also decrease P-gp activity. To investigate whether blank PEG-PE micelles have an influence on the intracellular ATP level, we measured the cytotoxocity of blank PEG-PE micelles to tumor cells and cellular ATP content. The blank PEG-PE micelles at different concentrations did not show any toxicity to MCF-7/ADR cells (Fig. 6a) and did not change the cellular ATP levels (Fig. 6b), indicating that the reduced P-gp activity was irrelevant with the cellular ATP content.

Effect of Blank PEG-PE Micelles on Expression of P-gp in MCF-7/ADR Cells

MCF-7/ADR cells were preincubated with 6.8 or 34 μM blank PEG-PE micelles for 48 h; the untreated

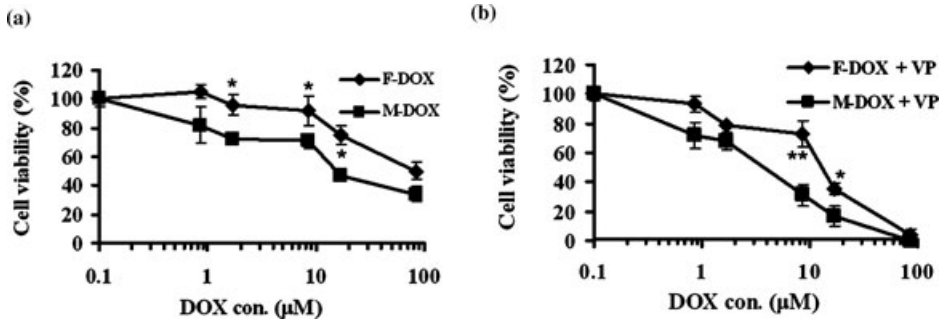

Figure 2. Cytotoxic effects of M-DOX in MCF-7/ADR cells. M-DOX enhanced cytotoxicity in the absence (a) or in the presence (b) of verapamil. Cells were exposed to various concentrations F-DOX or M-DOX with or without 10 μM verapamil for 2 h and then incubated in drug-free media for 72 h, cell viability was measured by MTT. Data represent mean ± SD (n = 3) for individual experiments. M-DOX significantly enhanced cytotoxicity compared with F-DOX ($^{*}P < 0.05$).

cells were used as a control. The 6.8 μM of blank PEG-PE micelles are comparable with the dose of DOX-loaded micelles used in the accumulation and retention experiments in this study, and the higher concentration is chosen for enlarging the effect of blank PEG-PE micelles reasonably. MDR-1 mRNA expression was analyzed using the RT-PCR assay and normalized with the β-actin mRNA levels. As shown in Figure 7a, blank PEG-PE micelles reduced the expression of *MDR-1* gene in a concentration-dependent manner. At the concentration of 34 μM, blank PEG-PE micelles markedly inhibited the transcription of *MDR-1* gene compared with the untreated sample. Thus in turn significantly reduced the expression of P-gp both in 6.8 and 34 μM blank micelles-treated cells ($P < 0.01$), as shown in Figures 7b and 7c. These results indicate that PEG-PE micelles alone can regulate the expression of *MDR-1* gene, which may contribute to the enhanced cellular drug retention.

Combination of M-DOX with siRNA Targeting *MDR-1* Gene to Improve Cytotoxicity

Combination of siRNA and chemotherapy has shown promising potential in cancer therapy. We chose *MDR-1* gene as a target, and combined this Geng's siRNA with M-DOX to inhibit the growth of MCF-7/ADR cells. First, 100 nM MDR-1 siRNA was transfected into MCF-7/ADR cells, and the transfection efficiency was evaluated at the both levels of mRNA and protein. As shown in Figures 8a–8C, the MDR-1 mRNA was significantly downregulated after 48-h transfection, and the P-gp expression was five times decreased than the untreated cells after 72-h transfection.

The cells were pretreated with 100 nM siRNA for 72 h and then treated with F-DOX or M-DOX for another 2 h, the combination of siRNA significantly increased cellular DOX fluorescence both for F-DOX and M-DOX, siRNA showed a similar effect to

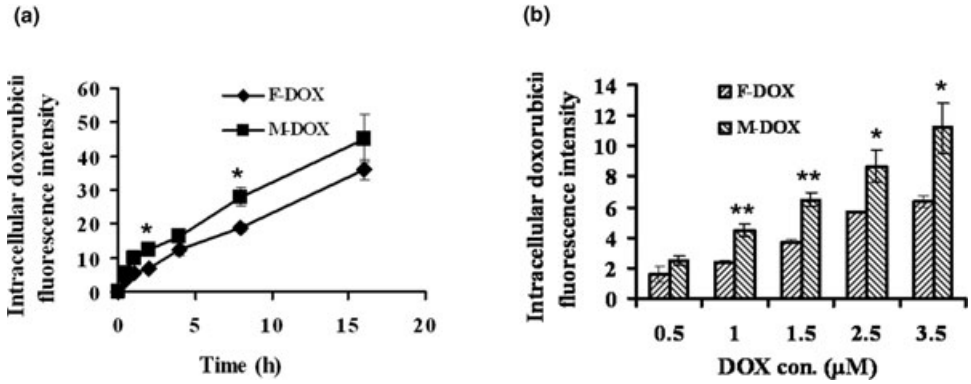

Figure 3. Time- and concentration-dependent internalization of M-DOX in MCF-7/ADR cells. Intracellular doxorubicin fluorescence intensity was detected by flow cytometry. (a) Cells were exposed to 1.0 μM of F-DOX or M-DOX for various hours. (b) Cells were exposed to F-DOX or M-DOX at various concentrations for 1 h. Data represent mean ± SD (n = 3) for individual experiments. M-DOX induces a significant increase in intracellular fluorescence compared with F-DOX ($^{*}P < 0.05$, $^{**}P < 0.01$).

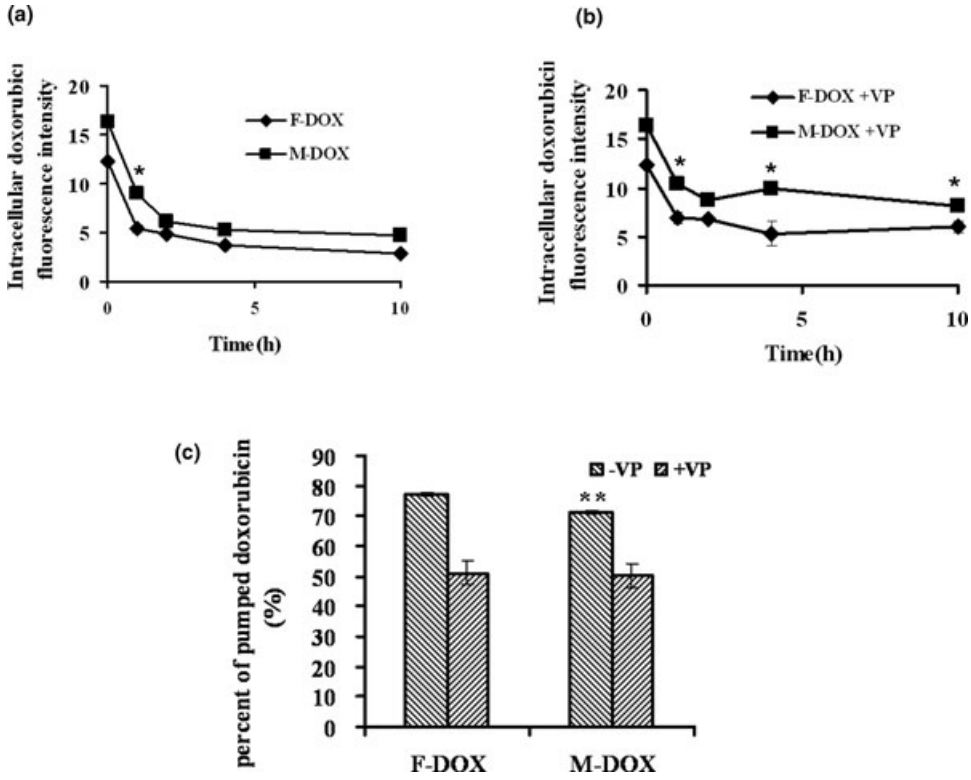

Figure 4. Time-dependent retention of M-DOX in MCF-7/ADR cells. Intracellular doxorubicin fluorescence intensity was detected by flow cytometry. Cells were exposed to 3.5 μM of F-DOX or M-DOX for 7 h, washed, and then incubated with drug-free media for different times in the absence (a) or in the presence (b) of 10 μM verapamil. (c) The percentage of intracellular DOX fluorescence intensity at 10 h to the initial fluorescence intensity. Data represent mean ± SD ($n = 3$) for individual experiments. M-DOX increases significantly the retention of intracellular fluorescence ($^{*}P < 0.05$; $^{**}P < 0.01$).

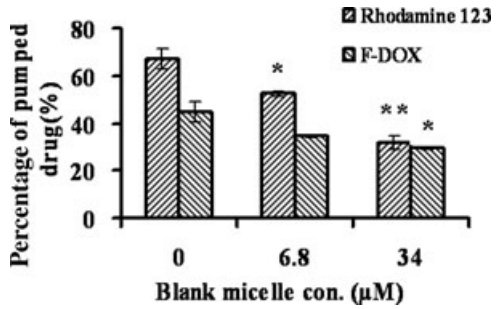

Figure 5. Effect of blank PEG-PE micells on P-gp activity in MCF-7/ADR cells. Intracellular fluorescence intensity was detected by flow cytometry. Cells were pretreated with PEG-PE micells for 48 h, and exposed to 500 nM Rhodamine123 or 17 μM F-DOX in the presence of 20 μM verapamil for 1 h, washed, and then incubated with drug-free media for another 1 h with or without 20 μM verapamil. The percentage of pumped drug is equal to one intracellular drug without verapamil/intracellular drug with verapamil. Data represent mean ± SD ($n = 3$) for individual experiments. Columns, mean; Bars, SD. Values significantly different from control cells were marked ($^{*}P < 0.05$; $^{**}P < 0.01$).

verapamil (Fig. 8d). Furthermore, the cytotoxicity of M-DOX to MCF-7/ADR cells was also detected in the presence of siRNA. The IC_{50} value of combining M-DOX with MDR-1 siRNA was 2.5-fold lower than that of M-DOX alone (Fig. 8e). These data suggest that the combination M-DOX with MDR-1 siRNA could be a useful approach to treat drug-resistant tumors.

DISCUSSION

The present study shows that the M-DOX can reach a higher cellular concentration within shorter time in the P-gp overexpressing MCF-7/ADR cells compared with F-DOX, indicating that M-DOX can internalize into cells more efficiently than F-DOX. This result was verified through DOX quantification by FCM and was also consistent with our total internal reflection fluorescence microscopy observation: the small vesicles with the red fluorescence of DOX appeared within 10 min (data not shown) in M-DOX-treated cells, whereas no fluorescent vesicles could be observed in F-DOX-treated cells at the same time.

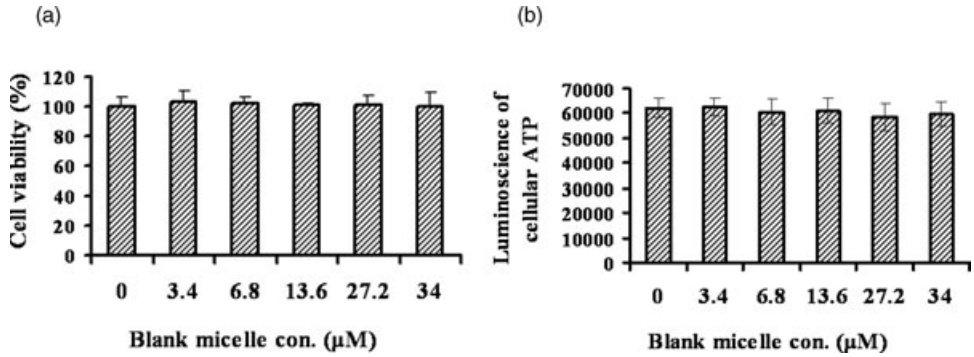

Figure 6. Effect of blank PEG-PE micelles on cell viability and ATP content in MCF-7/ADR cells. (a) Cell viability was detected by MTT. (b) Intracellular ATP content was determined by ATP assay kit after 48 h treatment with various concentrations of PEG-PE micelles. Data represent mean ± SD ($n = 3$) for individual experiments.

Importantly, we found that P-gp inhibitor verapamil had a less effect on cytotoxicity of M-DOX (Fig. 1f). Compared with in the absence of verapamil, in the presence of verapamil, the IC_{50} value of M-DOX was three times lower and the F-DOX was five times lower. In the absence of verapamil, the percentage of pumped M-DOX was decreased by 10% versus F-DOX, indicating that P-gp activity is partially inhibited by M-DOX, and PEG-PE molecules may have an influence on P-gp function. Previous studies have demonstrated that pluronics block copolymers molecules rapidly adhere to and incorporate into the cell membranes. This alters the structure of the lipid bilayers accompanied by significant decreases in P-gp ATPase activity.[30,31]

Our study showed that the depletion of cholesterol greatly increased intracellular M-DOX internalization (data not shown). It is known that cholesterol

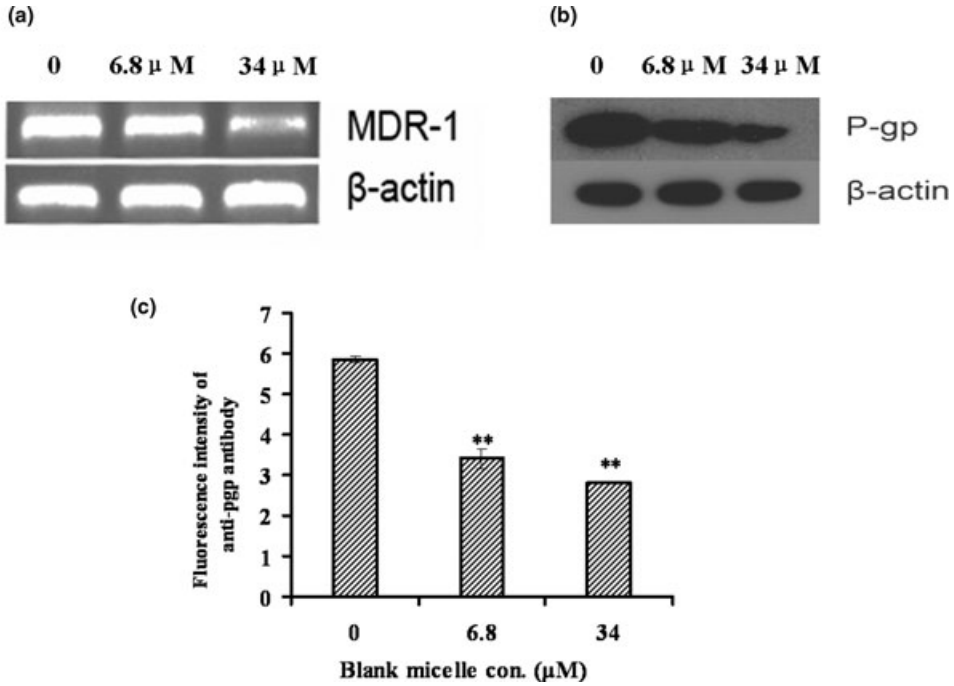

Figure 7. Effect of blank PEG-PE micelles on the expression of mRNA and protein of *MDR-1* gene. (a) Reverse-transcription polymerase chain reaction used to detect mRNA level of *MDR-1* gene and (b) western blot used to detect protein level of P-gp in MCF-7/ADR cells after 48 h treatment with 6.8 or 34 μM PEG-PE micelles. (c) P-gp expression was quantified by flow cytometry. Cells were exposed to 6.8 or 34 μM of PEG-PE micelle for 48 h. Cell surface was staining by FITC-conjugated anti-P-gp antibody. Data represent mean ± SD ($n = 3$) for individual experiments. Columns, mean; Bars, SD. Values significantly different from control cells were marked ($^{**}P < 0.01$).

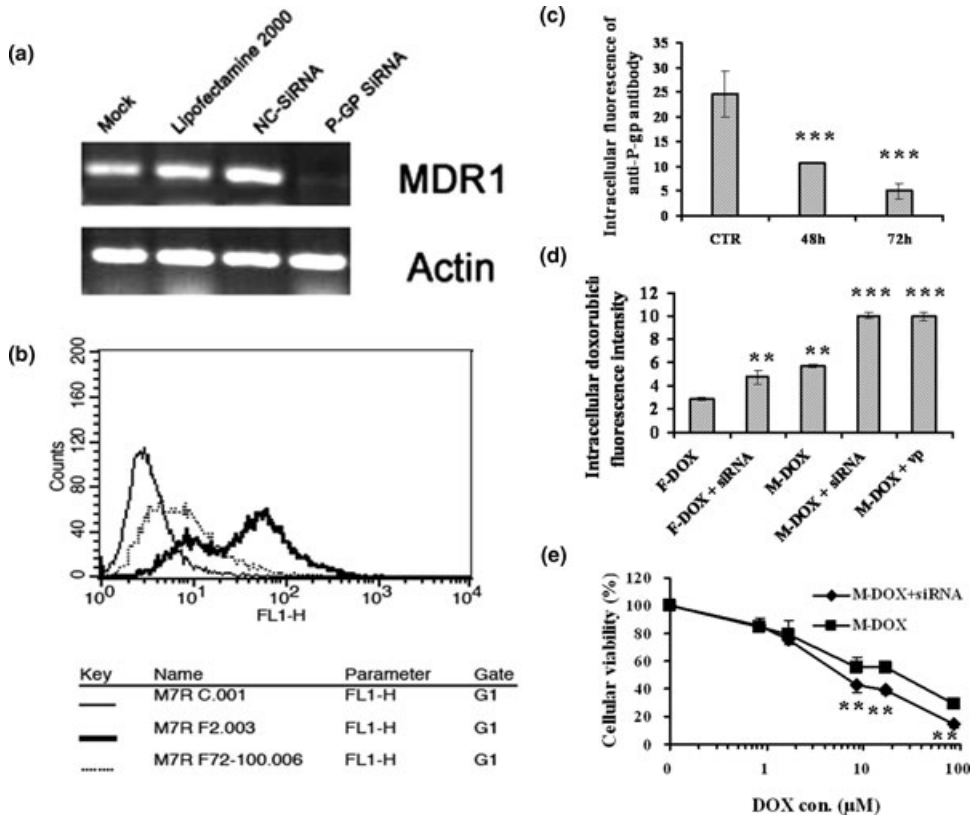

Figure 8. Effect of combining MDR-1 siRNA with M-DOX on cytotoxicity of DOX. (a) Reverse-transcription PCR-detected *MDR-1* gene expression after transfection of MDR-1 siRNA in MCF-7/ADR cells. Cells were transfected with 100 nM MDR-1 siRNA for 48 h, NC siRNA used as a negative control. (b and c) Flow cytometry analysis of P-gp expression after transfection of MDR-1 siRNA in MCF-7/ADR cells by surface staining of FITC-conjugated anti-P-gp antibody. Cells were transfected with 100 nM MDR-1 siRNA for 72 h (dashed line), untreated cells (bold line) and unlabeled cells (real line) were used as controls. (d) Flow cytometry analysis of intracellular DOX fluorescence after transfection of MDR-1 siRNA or treatment with 10 μM verapamil in MCF-7/ADR cells. Data represent mean ± SD ($n = 3$) for individual experiments. Columns, mean; Bars, SD. Values significantly different from F-DOX-treated cells were marked ($^{**}P < 0.01$). (e) Cytotoxicity of M-DOX combined with 100 nM MDR-1 siRNA for 72 h, untreated cells were used as a control. Data represent mean ± SD ($n = 3$) for individual experiments. Combination enhances M-DOX cytotoxicity compared with M-DOX alone ($^{**}P < 0.01$).

depletion removed P-gp from the raft membranes and reduced P-gp function in L-MDR1 cells, resulting in intracellular substrate accumulation.[31] Therefore, this may shed a light on the mechanism of M-DOX internalization.

On the basis of these finding as described above, we propose a hypothesis that PEG-PE block polymers may directly reduce the P-gp activity and enhance drug accumulation as well as cytotoxocity by extending cellular drug retention. To address this hypothesis, P-gp function and intracellular ATP concentrations were detected. We found PEG-PE had an inhibitory effect on P-gp function, which was through decreasing the level of mRNA and protein but not depleting intracellular ATP. This is different from pluronic block copolymers and lipid-based nanoparticles,[21] which inhibit P-gp function by depleting ATP or by inhibiting P-gp and depleting ATP. Fluorescent-labeled PEG-PE translocated into the mitochondria and Golgi after 12 h incubation (data not shown). PEG-PE may regulate P-gp expression through apoptosis-related pathways such as NF-κB pathway.

To further increase the antitumor efficacy, a combination study of P-gp-silencing siRNA and M-DOX was conducted; synergic administration of both agents showed superior inhibiting effect in resistant breast cancer cells. This two-step strategy integrated the advantages of siRNA technology and nano-sized drug delivery system to achieve a superior *in vitro* antitumor effect. Although *in vivo* study will involve more complex administration strategy, the combination of gene regulation and chemotherapy demonstrates a promising direction for future cancer therapy.[32] For

instance, a more advanced drug delivery system consisting both siRNA and M-DOX can be developed to achieve a sequent release of both agents within the same cell, and thus maximize the antitumor effect.

CONCLUSIONS

In brief, polymeric micelles consisting of PEG-PE and DOX were developed to treat resistant breast cancer cells. The main reason accounting for this enhanced retention is believed to be the efficient uptake of M-DOX by inhibiting P-gp mRNA and protein expression. Moreover, a combinative administration of silencing siRNA and M-DOX was proved to be a successful strategy in inhibiting the growth of MDR breast cancer cells.

ACKNOWLEDGMENTS

This work was supported by grants from State Key Development Plan Project (2006CB933305, 2007CB935801) the National Nature Sciences Foundation of China (No. 90606019, 30901869), National Science and Technology Special Project of Major New Drugs Creation (2009ZX09501-025)and China–Finland Inter-Governmental S&T Cooperation Project (2008DFA01510).

REFERENCES

1. Thomas H, Coley HM. 2003. Overcoming multidrug resistance in cancer: An update on the clinical strategy of inhibiting P-glycoprotein. Cancer Control 10(2):159–165.
2. Gottesman MM, Ludwig J, Xia D, Szakács G. 2006. Defeating drug resistance in cancer. Discov Med 6(31):18–23.
3. Higgins CF. 2007. Multiple molecular mechanisms for multidrug resistance transporters. Nature 446(7137):749–757.
4. Ozben T. 2006. Mechanisms and strategies to overcome multiple drug resistance in cancer. FEBS Lett. 580(12):2903–2909.
5. Sanfilippo O, Ronchi E, De Marco C, Di Fronzo G, Silvestrini R. 1991. Expression of P-glycoprotein in breast cancer tissue and in vitro resistance to doxorubicin and vincristine. Eur J Cancer 27(2):155–158.
6. Ling V. 1997. Multidrug resistance: Molecular mechanisms and clinical relevance. Cancer Chemother Pharmacol 40(Suppl):S3–S8.
7. Gottesman MM, Fojo T, Bates SE. 2002. Multidrug resistence in cancer: Role of ATP-dependent transporters. Nat Rev Cancer 2(1):48–58.
8. Wang Y, Yu L, Han L, Sha X, Fang X. 2007. Difunctional Pluronic copolymer micelles for paclitaxel delivery: Synergistic effect of folate-mediated targeting and Pluronic-mediated overcoming multidrug resistance in tumor cell lines. Int J Pharm 337(1–2):63–73.
9. Goren D, Horowitz AT, Tzemach D, Tarshish M, Zalipsky S, Gabizon A. 2000. Nuclear delivery of doxorubicin via folate-targeted liposomes with bypass of multidrug-resistance efflux pump. Clin Cancer Res 6(5):1949–1957.
10. Lee ES, Na K, Bae YH. 2005. Doxorubicin loaded pH-sensitive polymeric micelles for reversal of resistant MCF-7 tumor. J Control Release 103(2):405–418.
11. Mohajer G, Lee ES, Bae YH. 2007. Enhanced intercellular retention activity of novel pH-sensitive polymeric micelles in wild and multidrug resistant MCF-7 Cells. Pharm Res 24(9):1618–1627.
12. Dreher MR, Liu W, Michelich CR, Dewhirst MW, Yuan F, Chilkoti A. 2006. Tumor vascular permeability, accumulation, and penetration of macromolecular drug carriers. J Natl Cancer Inst 98(5):335–344.
13. Maeda H, Wu J, Sawa T, Matsumura Y, Hori K. 2000. Tumor vascular permeability and the EPR effect in macromolecular therapeutics: A review. J Control Release 65(1–2):271–284.
14. Nie S, Xing Y, Kim GJ, Simons JW. 2007. Nanotechnology applications in cancer. Annu Rev Biomed Eng 9:257–288.
15. Panyam J, Labhasetwar V. 2003. Biodegradable nanoparticles for drug and gene delivery to cells and tissue. Adv Drug Deliv Rev 55(3):329–347.
16. Torchilin VP. 2007. Micellar nanocarriers: Pharmaceutical perspectives. Pharm Res 24(1):1–16.
17. Buckingham LE, Balasubramanian M, Emanuele RM, Clodfelter KE, Coon JS. 1995. Comparison of solutol HS 15, cremophor EL and novel ethoxylated fatty acid surfactants as multidrug resistance modification agents. Int J Cancer 62(4): 436–442.
18. Coon JS, Knudson W, Clodfelter K, Lu B, Weinstein RS. 1991. Solutol. HS 15, nontoxic polyoxyethylene esters of 12-hydroxystearic acid, reverses multidrug resistance. Cancer Res 51(3):897–902.
19. Buckingham LE, Balasubramanian M, Safa AR, Shah H, Komarov P, Emanuele RM, Coon JS. 1996. Reversal of multidrug resistance in vitro by fatty acid-PEG-fatty acid diesters. Int J Cancer 65(1):74–79.
20. Komarov PG, Shtill AA, Buckingham LE, Balasubramanian M, Piraner O, Emanuele RM, Roninson IB, Coon JS. 1996. Inhibition of cytarabine-induced MDR1(P-glycoprotein) gene activation in human tumor cells by fatty acid-polyethylene-fatty acid diesters, novel inhibitors of P-glycoprotein function. Int J cancer 68(2):245–250.
21. Dong XW, Mattingly CA, Tseng MT, Cho MJ, Liu Y, Adams VR, Mumper RJ. 2009. Doxorubincin and paclitaxel-loaded lipid-based nanoparticles overcome mulitidrug resistance by inhibiting P-glycoprotein and depleting ATP. Cancer Res 69(9):3918–3926.
22. Minko T, Batrakova EV, Li S, Li Y, Pakunlu RI, Alakhov VY, Kabanov AV. 2005. Pluronic block copolymers alter apoptotic signal transduction of doxorubicin in drug-resistant cancer cells. J Control Release 105(3):269–278.
23. Minko T, Kopeckkova P, Pozharov V, Kopecek J. 1998. HPMA copolymer bound adriamycin overcomes MDR1 gene encoded resistance in a human ovarian carcinoma cell line. J Control Release 54(2):223–233.
24. Tang N, Du G, Wang N, Liu C, Hang H, Liang W. 2007. Improving penetration in tumors with nanoassemblies of phospholipids and doxorubicin. J Natl Cancer Inst 99(13):1004–1015.
25. Troost J, Albermann N, Emil Haefeli W, Weiss J. 2004. Cholesterol modulates P-glycoprotein activity in human peripheral blood mononuclear cells. Biochem Biophys Res Commun 316(3):705–711.
26. Borst P, Evers R, Kool M, Wijnholds J. 2000. A family of drug transporters: The multidrug resistance-associated proteins. J Natl Cancer Inst 92:1295–1302.
27. Cole SP, Bhardwaj G, Gerlach JH, Mackie JE, Grant CE, Almquist KC, Stewart AJ, Kurz EU, Duncan AMV, Deeley RG. 1992. Overexpression of a transporter gene in a multidrug-resistant human lung cancer cell line. Science 258:1650–1654.
28. Doyle LA, Yang W, Abruzzo LV, Krogmann T, Gao Y. 1998. A multidrug resistance transporter from human MCF-7 breast cancer cells. Proc Natl Acad Sci USA 95:15665–15670

29. Summers MA, Moore L, McAuley JW. 2004. Use of verapamil as a potential P-glycoprotein inhibitor in a patient with refractory epilepsy. Ann Pharmacother 38(10):1631–1634.
30. Batrakova E, Li S, Vinogradov S, Alakhov V, Miller D, Kabanov A. 2001. Mechanism of pluronic effect on P-glycoprotein efflux system in blood–brain barrier: Contributions of energy depletion and membrane fluidization. J Pharmacol Exp Ther 299(2): 483–493.
31. Batrakova EV, Li S, Alakhov VY, Elmquist WF, Miller DW, Kabanov AV. 2003. Sensitization of cells overexpressing multidrug-resistant proteins by pluronic P85. Pharm Res 20(10):1581–1590.
32. Sengupta S, Eavarone D, Capila I, Zhao G, Watson N, Kiziltepe T, Sasisekharan R. 2005. Temporal targeting of tumor cells and neovasculature with a nanoscale delivery system. Nature 436(7050):568–572.